NEHRP FINAL TECHNICAL REPORT, 2011

USGS External Grant G09AP00016

1. Regional Panel Designation: NC
2. Project Title: **Holocene Seismicity of the Northern San Andreas Fault: Refining the earthquake record with Precise Dating of Earthquake Triggered Turbidites**

3. Principal Investigators: Chris Goldfinger (PI)
COAS
Oregon State University
104 Ocean Admin Bldg.
Corvallis, OR 97331-5503
(541) 737-5214
(541) 737-2064 (fax)
email: gold@coas.oregonstate.edu

4. Authorized Institutional Representative Patricia A. Hawk, Interim Director of Sponsored Programs
Oregon State University
(541) 737-4933, (541) 737-3093 Fax
sponsored.programs@oregonstate.edu

5. Element Designation: Elements I, and III
6. Key Words Turbidites, Paleoseismicity, Neotectonics, Seismotectonics

7. Amount Requested: FY 2009: $ 45,875
8. Start Date: Jan. 1, 2009
9. Duration: 12 months (Jan. 1, 2009 - Dec., 31, 2009)
10. New or Renewal Project: New

NEHRP FINAL TECHNICAL REPORT, 2011

TITLE: Holocene Seismicity of the Northern San Andreas Fault: Refining the earthquake record with Precise Dating of Earthquake Triggered Turbidites

USGS External Grant G09AP00016

Chris Goldfinger, COAS Oregon State University 104 Ocean Admin Bldg. Corvallis, OR 97331, ph. (541) 737-5214 gold@coas.oregonstate.edu

Abstract

Earthquakes represent the largest releases of energy on earth. However, quantifying the temporal and spatial patterns of these great events remains elusive because our observations often span only one or even less than one seismic cycle. Paleoseismology has the potential to address these questions directly using a larger time span than available to geodesists and seismologists. This renewal proposal seeks to continue application of the paleoseismologic technique we have used in Cascadia to the turbidite history along the Northern San Andreas transform margin. New core data show that continental margin channels in Northern California have recorded a Holocene history of regional submarine landslides slides likely triggered by great earthquakes on the NSAF.

Thus far in our analysis of the data, we have first tested the turbidite record, applying multiple tests for synchronous triggering of turbidity currents. We have used ^{14}C ages, relative dating tests at channel confluences, and direct correlation of physical properties to determine whether turbidites deposited in separate channel systems are correlative, that is they were triggered by a common event. These tests can, in many cases, separate earthquake triggered turbidity currents from other possible sources. Turbidites along the Northern California margin have passed these tests well, and can be correlated with multiple proxies from site to site between Noyo Channel and the latitude of San Francisco. The evidence that the Holocene turbidite record is primarily an earthquake record, is now quite strong. Preliminary comparisons of our event ages with existing and in progress work at onshore coastal sites show correspondence to a remarkable degree, further circumstantial evidence that the offshore record is primarily earthquake generated.

New results also suggest a temporal and possible stress linkage to the Cascadia Subduction zone based on a number of near-coincident earthquakes over at least the past 3000 years. This temporal coincidence, with Cascadia event preceding the NSAF, strongly suggests triggering and therefore North-south directivity for many past NSAF earthquakes.

This project continues this effort, targeting the proxies that have been successful for event correlation, and adding several new techniques that are coming on line as effective tools for both

"fingerprinting" individual events, and for analysis of event chronologies with multiple timing constraints. There are few "smoking guns" in paleoseismology, thus our approach is to use multiple proxies to both test for earthquake origin, and to correlate events between separated sites. The original objectives of the project included following tasks:

• To acquire 30 AMS ^{14}C ages to focus on the latter half of the Holocene for best comparison with results from land sites. We planned to focus particularly on the most recent 5 events to help better define the timing of earthquakes that appear to have temporal correlatives in southern Cascadia. This analysis is focused on testing the Cascadia-NSAF stress linkage, and the implied N-S directivity or some NSAF earthquakes. In a parallel NSF project in Cascadia, we are refining ages for the most recent events along the southern Cascadia margin, using new core data. Triggering of the NSAF from Cascadia implies North-South directivity for some past NSAF earthquakes, carrying significant hazard implications for San Francisco and the Bay Area.

• We planned to use OXCAL to build age models for each key site along the margin, using both ^{14}C results, the timing constraints provided by hemipelagic sedimentation between events, and stratigraphic correlation constraints. OXCAL uses a Bayesian technique for refining event ages with multiple constraints which can be stratigraphic, historical or other timing, rate limiting, or correlation criteria.

• We planned to add XRF analysis to augment correlation of events using Gamma Density and very high resolution (3mm) magnetic susceptibility, and acquire additional very-high resolution data where needed. These are proxies for grain size, and have become mainstream tools for individual event correlation. We propose to include selected XRF analyses to strengthen the stratigraphic framework, and define stratigraphic boundaries. We will use principal component and Q-mode analysis of the XRF data to quantify this method, and to help define upper turbidite contacts.

This work has great societal relevance for the San Francisco Bay Area, where Holocene recurrence intervals for great San Andreas earthquakes are presently elusive. Working closely with land paleoseismologists, results from the turbidite record can address the long-term recurrence, possible patterns of recurrence, segmentation, and segment interaction along the Northern San Andreas. If we can better resolve the timing relationship with Cascadia, and thereby the potential stress linkage with the NSAF, the directivity of past NSAF events may be resolvable. This in turn has significant hazard implication for strong shaking in the Bay area (i.e. Aagaard et al., 2008).

FY 2009 Investigations Undertaken

Introduction and New Data Acquisition

When our original proposal was submitted in the Spring of 2008 and later supported in the fall of 2008 we expected this NEHERP project to continue as proposed using existing cores. Later that year, NSF invited new proposals for ship time in 2009, to which we responded. The result was a new cruise focused on southern Cascadia and the NSAF. As a result, we had a large number of new cores that were acquired in the Fall of 2009, and analysis was begun on those cores in parallel. We requested a no-cost extension to our NEHRP project so that analysis or both projects could be done in phase, and make best of use of the new data. The following is a

brief description of the new data collected on that cruise to outline the data added and available for analysis.

Cascadia NSAF 2009 cruise, R/V Thomas G. Thompson

From Sept. 30-October 15, we conducted a data collection cruise aboard the R/V Thomas Thompson in the southern Cascadia-northern San Andreas region. We had 12 working days for the sampling program along the continental slope of southern Cascadia and the Northern San Andreas Fault. We collected 22 Piston-trigger core pairs, 4 box cores, and 3 kasten cores, sampling lower slope basins and the filled trench of southern Cascadia, and also sampled channel systems on the Viscaino block south of the Mendocino escarpment and along the NSAF. We collected ~ 2000 line km of 3.5kHz Chirp sub-bottom reflection profiles and coincident multibeam bathymetry. We used the digital 3.5 kHz sub-bottom profiling and high resolution bathymetry to characterize each site and help refine core site selection. We clustered groups of cores as we did previously on the San Andreas and Cascadia margins. Pairs or groups of cores greatly improve the resolution of stratigraphic interpretation by providing replicates that corroborate observations from the site as a whole. Some trial and error was required to choose sites that offer optimal conditions, and expanded record, and which could be cored through the entire Holocene with the chosen coring gear. New data collected on this cruise along with existing data we have collected allowed relatively rapid determination of good sites and allow evaluation of the quality of the data at sea. At sea we visualized the data using the 3D ERDAS Imagine and ArcGIS 9.3 GIS systems, coupled with Fledermaus 3D visualization software to aid in pinpointing core sites.

While at sea we acquired point and loop magnetic susceptibility, Gamma density, P-wave velocity resistivity and high-resolution line scan imagery with a Geotek MST system (< 0.5 cm intervals). Gamma or CT density and magnetic susceptibility data were typically collected on orthogonal axes relative to a round core on the scanner track. This provides a crosscheck that signatures of a given interval are not the result of local 3D effects within the core. Post cruise, we completed scanning the cores with a newly acquired 64 slice CT scanner to examine the detailed turbidite structure to help resolve whether turbidites are separate events or multiple pulses in a single event, as well as illuminate coring artifacts and other relevant stratigraphic details at an unprecedented level of detail. This issue was less important in northern Cascadia with longer recurrence intervals and thick hemipelagic intervals, but along the southern Cascadia margin and the NSAF, recurrence times are shorter and hemipelagic intervals are thinner, resulting in more ambiguity in the stratigraphic record.

Radiocarbon Ages

We collected 27 new radiocarbon ages from cores on the northern NSAF (cores TT0909-13, 14 and 15PC/TC, 25KC and southernmost Cascadia (cores TT0909-01, 05, 06, 07, 09, and 10PC/TC). To date the age of emplacement of the turbidites, we extracted the calcium carbonate shells of planktic foraminifers preserved in the hemipelagic sediment below each turbidite. We sampled below each turbidite because the boundary between the top of the turbidite tail and the hemipelagic sediment is difficult to identify reliably. Hemipelagic sediment samples were freeze dried, washed in a dilute calgon (sodium hexametaphosphate) solution and sieved through a 63 μm stainless steel sieve, and then dried in a warm oven. 600–1,000 individual planktic foraminifers were identified to species level for dating. Radiocarbon ages were obtained using

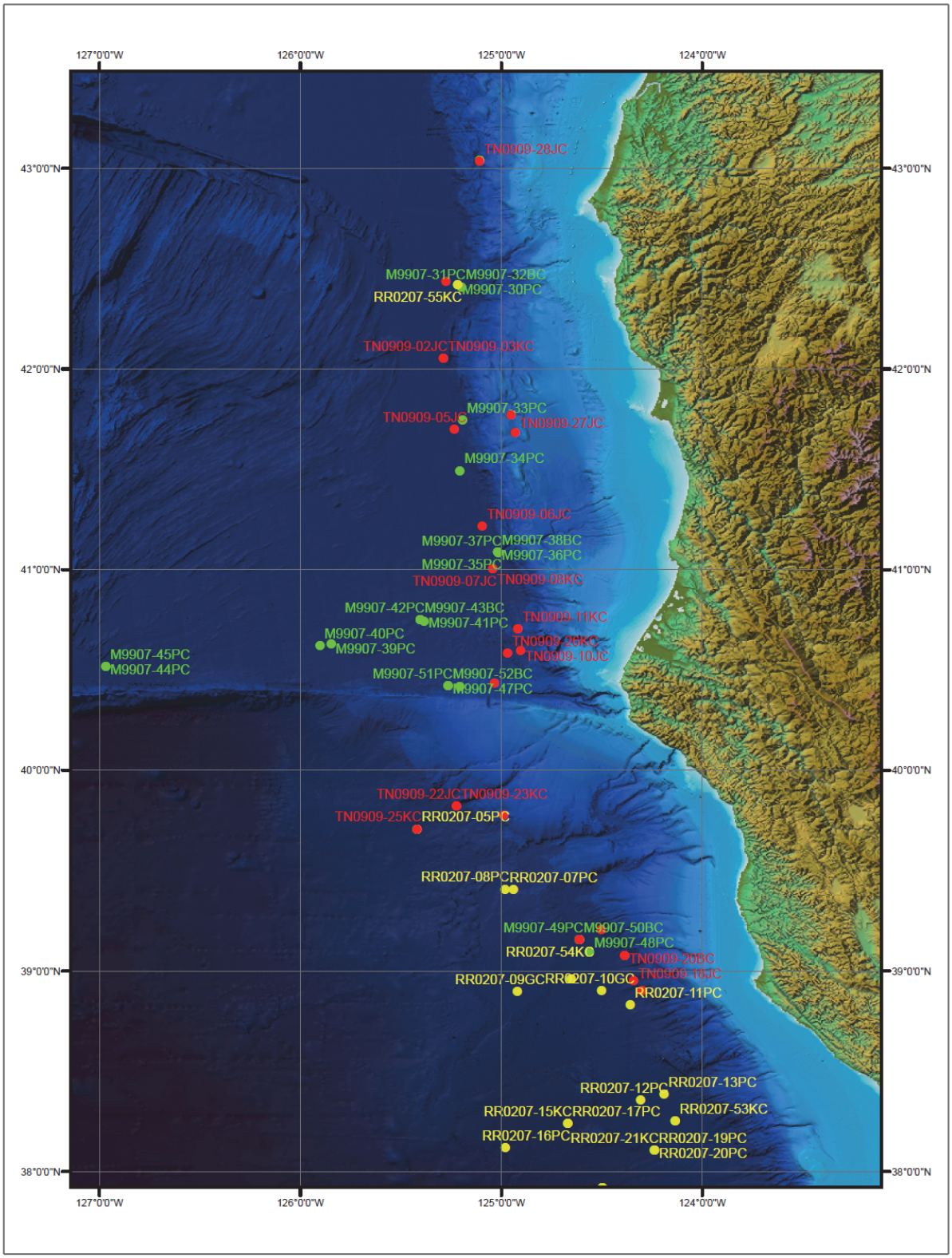

Figure 1. Core site map, southern Cascadia and NSAF region. Cores from three cruises are shown. Melville 1999 cruise (M9907 prefix) cores are in green, Revelle 2002 cruise (RR0207 prefix) cores are yellow, and 2009 cruise (TN0909 prefix are red.

Table 1. Radiocarbon data.

All samples are from the Archive and Working halves unless n						AMS		AMS age, peak		
Prefix	Samp. No.	Cruise No.	Core No.	Depth cm.	Sampling Notes	Age RCYBP	+ -	Calib 6.0 (1950) or	Range 1 sigma	Range 2 sigma
SCNSA	1	TN0909	01JC	13.5-16.5		4210	140	3775	3505 - 4020	3307 - 4326
SCNSA	3	TN0909	01JC	309-312		5260	70	5156	5056 - 5272	4910 - 5334
SCNSA	4	TN0909	01JC	431-434		6280	80	6302	6216 - 6387	6114 - 6486
SCNSA	2	TN0909	01JC	70-73		2790	80	2028	1915 - 2128	1835 - 2271
SCNSA	7	TN0909	05JC	299.5-302.5		4950	100	4802	4645 - 4943	4499 - 5119
SCNSA	6	TN0909	05JC	96.5-99.5	failed too small					
SCNSA	9	TN0909	06JC	168-171		2305	30	1508	1426 - 1570	1375 - 1655
SCNSA	20	TN0909	06JC	205.5-208.5	failed too small					
SCNSA	21	TN0909	06JC	216-219		2730	60	2014	1919 - 2106	1825 - 2218
SCNSA	10	TN0909	06JC	442.5-444.5		4710	45	4516	4420-4581	4327 - 4735
SCNSA	8	TN0909	06JC	59-62		1860	150	1063	918 - 1228	731 - 1351
SCNSA	18	TN0909	06TC	121-124		2400	35	1624	1549 - 1689	1493 - 1781
SCNSA	19	TN0909	06TC	222.5-224.5	Attempted Graphitization: failed too small					
SCNSA	16	TN0909	06TC	51.5-54.5		1550	50	751	672 - 805	646 - 892
SCNSA	15	TN0909	06TC	6.0-9.0		-175	50	BOMB CARBON		
SCNSA	17	TN0909	06TC	82-85		2050	70	1253	1170 - 1331	1058 - 1412
SCNSA	38	TN0909	07JC	112-115	Attempted Graphitization: failed too small					
SCNSA	39	TN0909	07JC	136-139	Attempted Graphitization: failed too small					
SCNSA	36	TN0909	07JC	161-164	Attempted Graphitization: failed too small					
SCNSA	35	TN0909	07JC	224-227	Attempted Graphitization: failed too small					
SCNSA	23	TN0909	07JC	31-34	Attempted Graphitization: failed too small					
SCNSA	22	TN0909	07JC	4.0-7.0		-120	25	BOMB CARBON		
SCNSA	55	TN0909	07JC	302.5-305.5	SENT					
SCNSA	57	TN0909	07JC	341.5-344.5	SENT					
SCNSA	50	TN0909	07TC	51.5-54.5	SENT					
SCNSA	51	TN0909	07TC	81.5-84.5	SENT					
SCNSA	24	TN0909	09JC	244.5-247.5		1640	20	844		
SCNSA	11	TN0909	09JC	269.5-272.5		1670	90	872		
SCNSA	25	TN0909	09JC	50.5-53.5		1060	45	366	304 - 418	270 - 469
SCNSA	37	TN0909	10JC	124-127	Attempted Graphitization: failed too small					
SCNSA	34	TN0909	10JC	134-137		1345	20	587		
SCNSA	12	TN0909	10JC	267-270		1800	60	1012	926 - 1076	873 - 1177
SCNSA	31	TN0909	10JC	295-298		1700	25	906		
SCNSA	32	TN0909	10JC	306.5-308.5	Attempted Graphitization: failed too small					
SCNSA	33	TN0909	10JC	313.5-315.5		2310	60	1526		
SCNSA	26	TN0909	10JC	53-56	Attempted Graphitization: failed too small					
SCNSA	13	TN0909	14JC	12.5-15.5		1250	50			
SCNSA	14	TN0909	14JC	269-272		5700	70			
SCNSA	27	TN0909	14JC	36-38.5		1750	60	959		
SCNSA	28	TN0909	14JC	518-521		11910	300	13033		
SCNSA	29	TN0909	14JC	532-535		12370	60	13468		
SCNSA	30	TN0909	14JC	542-545		12580	90	13676		
SCNSA	43	TN0909	25KC	274.5-276.5	SENT					
SCNSA	45	TN0909	25KC	42-44	SENT					

60 samples total have been taken from cores
27 samples have been run successfully
11 samples failed
6 samples are currently at UCI for dating
10 samples do not have enough to run
6 samples have not yet been processed

accelerator mass spectrometry (AMS) methods at the Keck AMS facility at University of California, Irvine, in collaboration with John Southon.

The radiocarbon dates are reported with 2-sigma lab error (Stuiver and Polach, 1977). Lab errors were generally much lower from the UC Irvine lab, averaging ±20 RC years. Lab errors with radiocarbon dating are straightforward and based on counting statistics from the laboratory. All dates are calibrated with Marine04, and in many cases we made additional corrections to the raw and calibrated dates, including the reservoir correction, sediment sample thickness correction, and a correction for differential erosion (derived from multiple cores at one site) in some cases. Our aim is to arrive at the closest age to the date of emplacement, which will most likely be a close maximum limiting age.

We also calculated event ages based on hemipelagic thickness above and below undated turbidites using smoothed sedimentation rates, introducing observational error at that stage. For individual dates, we propagated these uncertainties using RMS (root mean square) calculations using estimates of the uncertainties at each step. This calculation included the lab uncertainties, and resulted in the final reported 2σ range for each radiocarbon age. We use ages computed from OxCal, a Bayesian Markov Chain Monte Carlo calibration and age model software package (Ramsey, 2001). To compute event ages, radiocarbon and hemipelagic ages (as computed with the above described RMS errors) of well-correlated beds are "combined" to estimate depositional ages where the probability density functions (PDF's) of the radiocarbon ages and hemipelagic ages are combined to compute a new probability function for each turbidite, with narrower 2 sigma ranges based on Bayes theorem. The prior assumption of the Bayesian calculation is that we have correctly correlated the turbidites stratigraphically. OxCal also tests the assumption of coevality (as the resolution of radiocarbon) with several statistical tests (χ^2 and Acomb). All correlated beds combined in this way pass these tests. Nevertheless, radiocarbon may not be able to distinguish between a closely spaced series of bed emplacements temporally.

Faunal data were collected from planktic sample assemblages. The close correspondence in dates between land and marine ages, and across marine sample sites observed in both Cascadia Basin and along the NSAF suggests that, overall, neither bioturbation (Wheatcroft, 1992; Smith et al., 1993; Thomson and Weaver, 1994; Thomson et al.,1988) nor basal erosion significantly biases ^{14}C dates derived from planktic foraminifers. Analyses of foram test size, species specificity and other potential biases for Cascadia are presented in Goldfinger et al. (2012).

Not all intervals were directly datable by this method. As foraminifer abundance is much lower in the latest Holocene (in some cases we found abundances as low as five individuals/cc), samples representing times younger than ~2,000 cal yr B.P. were difficult to date. The total volume of material available was limited by the hemipelagic sediment deposited between turbidites, thus shorter recurrence intervals (in southern Cascadia and the NSAF) also reduced the chances of obtaining one or more successful ^{14}C dates. In the age range of ~ 2,000–300 cal yr B.P., it was sometimes necessary to combine samples from piston and trigger cores, and rarely, from multiple localized pairs of piston and trigger cores to collect the required minimum of ~1.0 mg carbon (~600–1,000 specimens) for a successful date. In some cases, we collected multiple cores and a jumbo kasten or box core for this purpose in anticipation of dating difficulties. Mixing in this way requires perfect correlation between the local core sets, though when done incorrectly, incongruous ages were the result.

CT scanning

Cores from southernmost Cascadia and the NSAF were imaged with an Aquilion 64 CFX Computer Tomographic (CT) imager. This includes the previously collected 2002 NSAF cores. This device uses a 64-row Quantum detector for simultaneous 64-slice scanning with voxel spatial resolution of 0.35 mm and volume-imaging capabilities. The Toshiba Aquilion 64 CT system is optimized for low-contrast medical applications, making it ideal for subtle stratigraphic relationships in soft sediment. We have used the imagery to improve understanding of the stratigraphic sequence, as it easily images the smallest details of turbidite structure and also reveals coring artifacts, liquefaction, the boundaries between hemipelagic sediment and turbidite tails bioturbation. CT imagery provides as many slices of the core volume, in any orientation, as needed to interpret the stratigraphy and depositional sequence. It allows the user to avoid coring artifacts to look at each deposit from enough angles that most difficulties can be resolved by simply viewing the unit from another angle. The system is in every way analogous to 3D seismic imaging, uses similar software, and allows similar detailed investigation of the stratigraphy at sub-millimeter scale. CT imaging allows the 0.37 mm resolution voxel volume to be sliced and viewed in any orientation, allowing the interpreter to view the internal details of cross bedding, erosion and relationship between units and sub-units.

High-resolution CHIRP reflection profiles

Our proposal did not include any collection or analysis of sub-bottom seismic profiles. However, these profiles are now available, collected on our 2009 cruise, and allow tracking of turbidite stratigraphy along strike both in southern Cascadia and the Northern San Andreas, a significant boon to inter-site core correlation. The continuous 3.5 kHz sub-bottom profiles were collected with a Knudsen 320 BR (FM chirp mode sweeping 2 to 6 kHz) at full bandwidth and data rate. These lines were heave-corrected in real time using the ships PosMV320. We thus have a complete set of survey lines along the trench axis, with a number of partial strike lines, as well as longitudinal lines through and connecting the slope basin sites. These lines imaged individual turbidites in the Holocene section in 1200-3100 m water depth. Digital correlation processing of the Chirp signal reduces the effective frequency, improving the signal to noise ratio and boosting the effective vertical resolution to about 25cm, degraded somewhat by off-axis scatterers and the water column. We are able to image individual turbidites separated by 20-30 cm. These data add seismic-stratigraphic correlation to the suite of tools we will employ to build the stratigraphic framework for inter-site correlation.

We post-processed the 3.5 kHz reflection data using Sioseis (http://sioseis.ucsd.edu/sioseis.html; Henkart, 2006) to develop depth sections from the SEG-Y envelope data, using the 1 cm P-wave and density data from the cores for the conversion of time to depth. We generated synthetic seismic sections and made velocity adjustments to the model to match the typically slightly higher velocities of the real section as compared to lab measurements (Abrams et al., 2002). We used intersite correlation of the seismic sections and synthetics to test similarity (or not) of the shallow turbidite sections, extending to the typical 30-50 m depth of the sections.

Core Correlation

Correlation between sites was conducted by integrating physical property parameters with core imagery, age data, and CT data and interactively testing alternate correlations. Our methods have evolved significantly since the earlier efforts along the NSAF. We now make extensive use

of very high-resolution CT data, and greater used of smear slides and grain size analysis. To integrate the data, we now make greater use of industry stratigraphic correlation techniques as well.

Detailed understanding of the stratigraphy at most sites was improved by acquiring multiple cores at each site when possible. Locally, the stratigraphy and its local variability could be well constrained with 2-3 piston-trigger pairs of cores, and differential basal erosion could be detected and quantified by comparing individual hemipelagic intervals across the core set (Goldfinger et al. 2012; Pastor et al., 2009). This reduced the possibility of correlating an unrepresentative example of a given event, and allowed for improved assessment of basal erosion, missing tops, and core deformation across the core set at each site, commonly providing at least one uneroded and undeformed example of each event. With addition of the new 2009 cores, we were able to use this method on the NSAF cores as well, which previously did not have enough local replication to treat the sites in this way.

The correlation procedure we used is to match tops and bases of individual beds using all data simultaneously, a procedure known as "flattening". The combined data set from the turbidite sequences are shifted iteratively relative to each other, using "ghost traces" to compare alternative detailed matching of wiggle traces from site to site, similar to e-log correlation in the oil industry (McCubbin, 1982; Lovlie and Van Veen, 1995; Chen et al., 2009). These methods have also been applied in academic research with piston, gravity and ODP/IODP cores (e.g. Fukuma, 1998; Karlin et al., 2004; Abdeldayem et al., 2004; Abrams, 2002; St-Onge et al., 2004; Iwaki et al., 2004; Schnellmann et al., 2002; Goldfinger et al., 2008, 2012).

In addition to correlation of cores in local groupings, we found it possible to correlate unique physical property signatures of individual turbidites between cores at greater distances, and between isolated sites with no physical connection (Goldfinger et al., 2008, 2012). Cascadia and NSAF turbidites are typically composed of multiple stacked and truncated fining-upward sequences (Bouma A-C) capped by a fine-grained fining upward tail associated with waning of the turbidity current (Bouma D). The magnetic susceptibility, density, and grain size trends within each event are closely correlated allowing the use of high-resolution density and magnetic data as grain size proxies in many cases, though this must be verified with each lithology (Goldfinger et al., 2012). These turbidite "fingerprints" formed the basis of along strike correlations, closely supported by ^{14}C ages reported extensively in Goldfinger et al. (2012).

In detail, the magnetic susceptibility (MS) signal is associated with terrestrial silt-sized magnetic minerals, though sand is usually present at the turbidite base (see Stupavsky et al., 1976, King et al., 1982). The sand may be non-magnetic quartz grains, so the MS peak does not always precisely correlate with a maximum of grain size. Nevertheless the approximation is reasonable in most cases (using both Gamma and CT density with MS reduces this problem). These "fingerprints" therefore represent detailed depositional grain size time histories of each turbidite.

Core Stratigraphy and Sedimentology

We performed detailed grain size analysis and microscope work on individual turbidites, focusing on the smaller mud turbidites in southern Cascadia, and the upper beds for the NSAF. The hypothesis of stress triggering of the NSAF requires more detailed knowledge of both the

NSAF turbidites, and of the southern Cascadia turbidites, including the so-called "mud-turbidites", or thinner finer grained beds that have been proposed as additional southern Cascadia earthquakes.

We determined hemipelagic thickness and mud turbidite boundaries using primarily visual observations of color change, X-radiography and CT imagery, and high-resolution physical property data (see Goldfinger et al., 2012), augmented with smear slide photomicrograph transects across key boundaries where required. High-resolution gamma density, point magnetics and CT imagery proved the most sensitive and reliable, acting as proxies for grain size as previously described, however this method must be verified for applicability with specific lithologies. In ideal cases, both density and magnetic susceptibility values declined upward in the fining upward tail, and reached an inflection point at which constant values continued upward to the base of the overlying turbidite, reflecting a homogenous uniform grain size and lithology in the hemipelagic sediment. The density and susceptibility curves were verified by grain size analyses to confirm this relationship. In numerous examples, many hemipelagic-tail boundaries could be accurately identified by this method, which was corroborated with color change observations for most cores. The primary difficulty with this method proved to be bioturbation, which blurs the tail boundary, an effect that was evident in the physical property and CT data. Using grain size analysis directly was not always as diagnostic as desired, and practically limited by the large numbers of samples required for regional analysis of many cores. Grain size transects across key problematic boundaries were run with a Beckman-Coulter LS 13-320 Laser diffraction particle size analyzer (Blott and Pye, 2006). Combined with smear-slide grain counts for lithic and biogenic components, a good result could be obtained, though silicious biogenic fragments sometimes were larger than the lithic component in hemipelagic sediment, and therefore generated somewhat noisy results.

Results

Nature and Origin of Southern Cascadia and NSAF turbidites

An important consideration for turbidite paleoseismology is the origin of the turbidites, which can come from several sources. As part of this project we collected smear slide transects from a number of cores to look for evidence of the water depth at the origin of the submarine slides that transformed into turbidity currents. Smear slides taken in a transect across Cascadia event T5a and several other beds at Rogue Canyon show the lithic content contrast between T5a (upper two slides) with 40-60% lithic fragments and the thin interval of hemipelagic sediment below with 20-30% lithic (lower two slides). The biogenic material in the tail of T5a is rich in heterogeneous patches of glass sponge spicules transported from shallower water. The hemipelagic material contains intact large and fragile spherical radiolarians, common in the hemipelagic intervals and rare to absent in the mud-silt turbidites. This typical bed shows the shift from dominant biogenic material in the surrounding hemipelagic sediment to lithic fragments. The biogenic material included in the tail of this typical bed is rich in glass sponge spicules, making up as much as 50% of the turbidite tail in some samples. The glass sponges generally live at depth ranges of 150–1300 m (Bett and Rice, 1992; Tunnicliffe et al., 2008). These sponges have been observed at several Cascadia canyon heads, notably Grays Canyon, on

flat plateaus flanking the canyon rim (Paul Johnson and Elizabeth Clarke, unpublished data). The Rogue Apron cores are all at depths of ~ 3100 m, far deeper than the sponge habitat, and therefore the spicules were likely transported to the Rogue Apron by turbidity currents from the mid slope region.

Correlation of southern Cascadia turbidites to the Mendocino Triple Junction

New cores collected in 2009 have, along with Chirp reflection profiles, offered additional data with which to evaluate continuity of turbidite beds southward from Rogue Apron beyond the interpretation presented in Goldfinger et al. (2012). Correlation and dating of these beds is integral to our investigation of the stress relationship to the NSAF, as they are inferred to be the result of southern Cascadia earthquakes which have been temporally linked to the temporal record of NSAF earthquakes (Goldfinger et al., 2008).

In all, 29 new piston and Kasten cores were collected aboard the R/V Thompson between Rogue Apron and Noyo Canyon just south of the Mendocino Triple Junction. Here we present new data between Rogue Apron and Trinidad Plunge Pool integrated with the data presented in Goldfinger et al. (2012). Bed correlation along this section of the margin proved to be more robust than previously reported due to the increased spatial density of cores, additional age control and stratigraphic constrains provided by high-resolution chirp reflection profiles.

The new cores in the Rogue –Trinidad section of the proximal abyssal plain include six piston-trigger core pairs and one kasten core, 13 cores in all. These cores are 01, 02, 04, 05, 06, and 07 JC-TC, and 03KC (A new designation "jumbo core" is used for post 2007 cores, but these are identical piston cores designated "PC" in earlier publications (see **Fig. 1** for locations). We focus on the better of these cores, 01, 02, 05, 06, and 07 JC/TC. Cores 03KC and 04JC each have missing section, heavy bioturbation, or core deformation that make interpretation difficult. Cores 02 and 07JC currently have no age control, but are relatively straightforward to correlate to neighboring cores (above ~ 3000 cal BP for 07JC). Additional cores south of Trinidad Plunge pool are more difficult to correlate stratigraphically, have limited age control, and are not included in the preliminary results reported here. Cores inside the Trinidad Plunge Pool, reported in Goldfinger et al. (2012) are somewhat less straightforward than the newer cores presented here. Below ~ 800 cal BP, the plunge pool cores are well correlated to those outside the plunge pool. From 0-800 cal BP, numerous beds are present in the section that are not found outside the plunge pool, a discordance that remains unresolved (Goldfinger et al., 2013). Generally, cores 01-06 PC TC all contain clear and distinct turbidite sequences. Core 01 JC/TC,

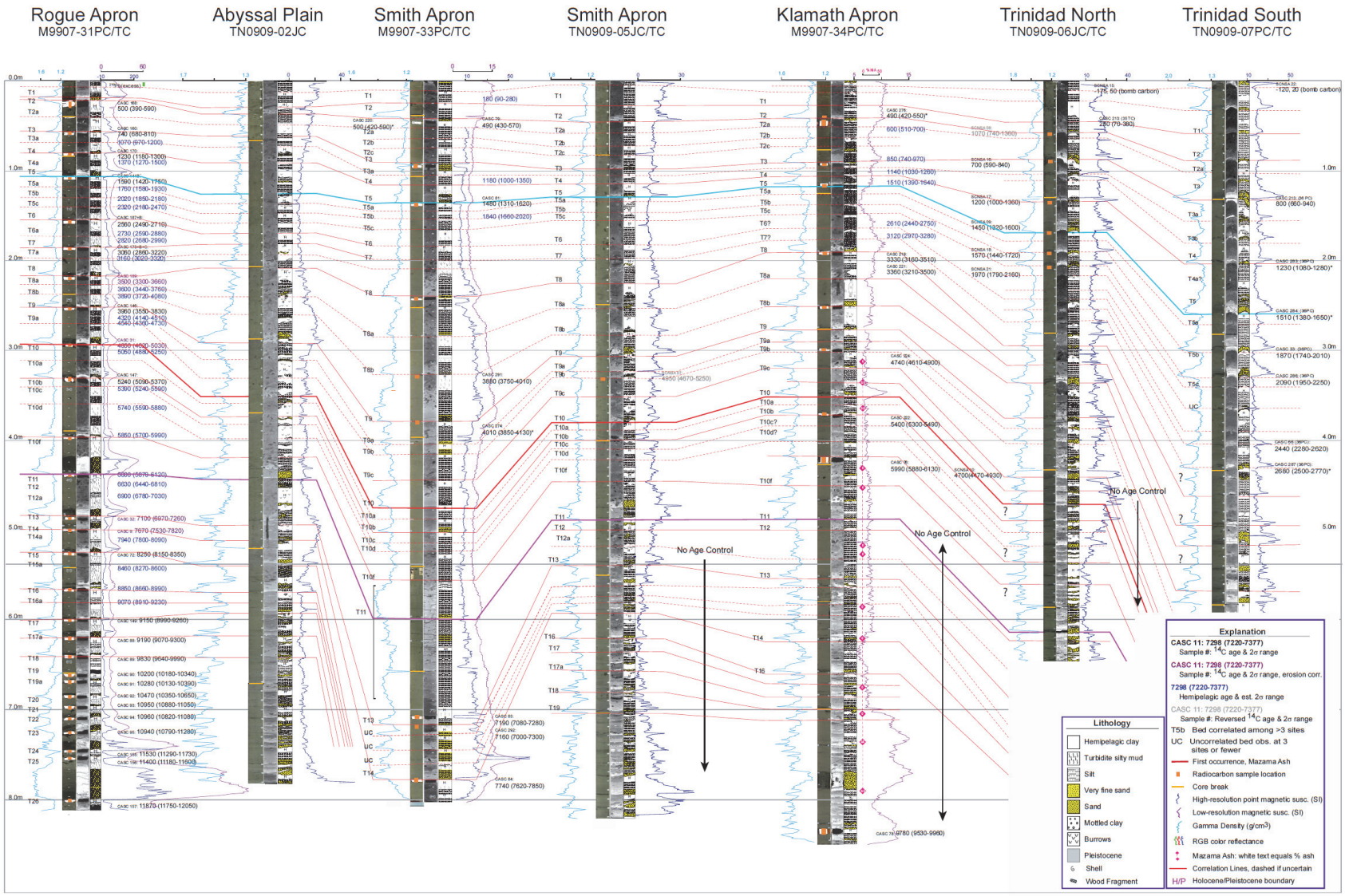
Rogue Apron
M9907-31PC/TC
Abyssal Plain
TN0909-02JC
Smith Apron
M9907-33PC/TC
Smith Apron
TN0909-05JC/TC
Klamath Apron
M9907-34PC/TC
Trinidad North
TN0909-06JC/TC
Trinidad South
TN0909-07PC/TC
No Age Control
No Age Control
No Age Control
Lithology
Hemipelagic clay
Turbidite silty mud
Silt
Very fine sand
Sand
Mottled clay
Burrows
Pleistocene
Shell
Wood Fragment
Explanation
CASC 11: 7298 (7220-7377)
Sample #: 14C age & 2σ range
CASC 11: 7298 (7220-7377)
Sample #: 14C age & 2σ range, erosion corr.
7298 (7220-7377)
Hemipelagic age & est. 2σ range
CASC 11: 7298 (7220-7377)
Sample #: Reversed 14C age & 2σ range
T5b Bed correlated among >3 sites
UC Uncorrelated bed obs. at 3 sites or fewer
First occurrence, Mazama Ash
Radiocarbon sample location
Core break
High-resolution point magnetic susc. (SI)
Low-resolution magnetic susc. (SI)
Gamma Density (g/cm3)
RGB color reflectance
Mazama Ash: white text equals % ash
Correlation Lines, dashed if uncertain
H/P Holocene/Pleistocene boundary

Figure 2. Turbidite correlation along ~130km of the southern Cascadia margin from Rogue Apron to the Trinidad Plunge Pool. Turbidites with sandy bases shown in solid lines, silty and mud turbidites shown in dashed lines. Three turbidites, T5, T10, and T11 are color coded to match the corresponding seismic reflectors in Figure 8. Depth of key reflectors is compatible with the trends in the seismic section (though definitive correlation is not possible) after velocity correction: deepening at Smith, then shallowing slightly before deepening significantly near Trinidad Plunge Pool. Many of the Rogue mud turbidites appear to thicken and coarsen southward, as do most of the margin wide turbidites, with the exception of T4, T6, T7 and T8, which thin southward (interpreted T numbers assigned to beds after final correlation). Tentative correlations unsupported by age control shown in gray. Modified with additional data after Goldfinger et al., 2012, their Fig. 44b.

located 5 km seaward of our original 1999 cores on Rogue Apron, correlates directly to those cores with little variation. This new core offers improved definition of the Rogue stratigraphy, as CT data was collected for this core prior to any sampling. The oldest regional event in the Holocene turbidite section correlated in Goldfinger et al. (2012), like the earlier cores, is marked by regional event T18, the base of which is found at 780 cm below the core top. The same bed in the more proximal M9907-30 and 31PC/TC is found at 635 cm, indicating a ~ 20% seaward thickening of the Holocene section. We attribute this to a greater capture of the middle grain sizes of the turbidite tail in the more distal cores. The more proximal cores exhibit significant bypassing of the middle grain sizes (Kneller and Buckee, 2000; Stevenson et al., 2012) at those sites based on common sharp upper contacts between the coarse-grained phases and the fine-grained turbidite tail. These gaps in grain size distribution are less apparent or absent at the more distal 01JC/TC site, making up the thickness difference between the two sites (Goldfinger et al., 2013).

Moving southward, new cores 02 and 05 JC/TC and 03 KC, along with older cores M9907 33PC and M990734 PC, are located along a part of the margin fed only by smaller or no canyon systems. Perhaps not coincidentally, the turbidite beds have reduced grain size profiles, and greater bioturbation, although the overall Holocene section thickness is moderately expanded (expanded below ~ 3500 cal BP, and compressed above that age). We estimate a ~ 25% increase in overall thickness in this area relative to the Rogue Apron core 01JC based on correlation of key horizons. Further to the south, beginning at ~ 41.7 N at the site of M9907-34PC, the section decreases in thickness to minimum, then begins to increase southward with an attendant increase in calibrated gamma density and basal grain size in correlative beds. At approximately 41.2N, near the site of TN0909-06JC/TC, correlation of key beds indicates a thickening section, which increases further to 180-200% of the Rogue Apron values at 41.02N, the site of TN08909-07PC/TC. The variation in section thickness is corroborated by Chirp reflection profiles. Most of this thickness increase can be attributed to nine additional beds that appear in the section younger than 4800 cal BP, mostly toward the southern end of the region between Rogue Apron and Trinidad Plunge Pool. Six of these beds are below the likely AD 1700 turbidite, while three are younger, and are discussed below (Goldfinger et al., 2013). These beds have sharp bases and fining upward sequences, but are not correlated over large enough distances or linked to onshore paleoseismic sites, thus their origin is presently not testable. We see no coherent increase in bed thickness southward for most beds, despite a clear density and grain size increase.

In addition to the increase in overall section thickness, grain size profiles for most beds coarsen southward, both for beds correlated to sandy turbidites at Rogue Apron, and for those correlated with mud turbidites at Rogue. For example, regionally correlated beds T1-T11 extend

at least southward to Trinidad Pool. Older beds may also be correlable, however interpretation below that depth is hampered by increasing turbidite frequency, lack of hemipelagic intervals for datable material, and other factors as discussed in Goldfinger et al. (2012), thus we focus on the latter half of the Holocene. Not all beds increase in density and grain size southward however. Regionally correlated beds designated T1, T4, T7 and T6 at Rogue Apron diminish in density and grain size southward, bucking the regional trend and making correlation of adjacent beds less robust. The largest regional beds, T11 and T16 also diminish southward. Regional beds T2, T3, T5, T5b, and T5c become more prominent southward, to an extent greater than the regional trend. Many other beds show local variability while generally following this trend. An extreme example is T11, which at Smith Apron (M990733PC) apparently expands to ~ 1.2 m in thickness, and appears to coarsen upward. Beds T4 and T5 are also anomalously coarse and thick in M9907-36PC (Trinidad Plunge pool, Goldfinger et al. 2013).

In the well correlated section younger than ~ 4800 years, of particular interest is the along-strike correlation of the 13 Rogue mud turbidites in that time window, T2a, T3a, T4a, T5a, T5b, T5c, T6a, T6b, T7a, T8a, T8b, T9a and T9b. Limited radiocarbon data from the southern core sequence support our preferred correlation as of this writing, but with additional radiocarbon data, other interpretations may also prove to satisfy the data.

Discussion

Southern Cascadia

Stratigraphic correlation of individual beds among separated sites offers a test of event synchroneity, particularly in cases where sites are isolated from each other, and isolated from shallow water and terrestrial sediment sources. Although never absolute, a close correlation of detailed stratigraphy, combined with age compatibility from both radiocarbon and time calculated from hemipelagic sedimentation (at the resolution of radiocarbon), form a strong case for synchronous deposition at separated sample sites.

The evidence for the thinner mud-silt turbidites and along-strike correlation lies in the aggregate of information, including the sedimentology of the beds, the continuity of regional stratigraphy based on core and seismic stratigraphy, the temporal stratigraphic correlation between sites, and the possible links to Bradley Lake and the coast range lakes of southern Cascadia. Unequivocal evidence of earthquake origin does not exist, however this is relatively normal in paleoseismology, and geology in general, where airtight smoking guns are rare.

The detailed geophysical "fingerprinting" of turbidites through their grain size proxies has direct implications for testing synchronous deposition. Goldfinger et al. (2007; 2008; 2011; 2012) and Patton et al. (2009) show that tracking individual deposits through their physical property signatures, combined with stratigraphic details revealed in CT imagery and direct observation can form the basis for positive stratigraphic correlation. When supported by consistent (though rarely diagnostic) radiocarbon ages, it is feasible to interpret the deposits as resulting from the same event, establishing synchroneity along strike.

That such grain-size "fingerprints" exist suggests that triggering mechanisms that produced them, or influences such as hydrodynamics or physiography must have some commonality, as producing matching grain size patterns in multi-pulse turbidites by coincidence is unlikely. The correlative patterns must be reproduced in multiple canyon/channel systems, and ideally in

isolated settings with no sources of terriginous input or shallow water influence by storm waves or tsunami. Detailed stratigraphic fingerprinting is a relative dating test, where synchronous deposition or lack thereof may be tested, and is independent of absolute dating techniques and the inherent errors involved in their use.

The equivocal evidence in some of the smallest of these beds can be attributed to bioturbation, and possibly due to reduced efficacy of the geophysical grain size proxies at very small grain sizes. Bioturbation plays a much greater role in overprinting sediment stratigraphy for the smaller beds. The large turbidites are much less disturbed by bioturbation, probably because the benthic infauna was smothered by the rapid influx and burial event, where the smaller turbidites likely did not bury and kill the local infauna. For the smaller beds, the effect may have been just the opposite, bringing enough nutrients to abyssal settings to actually cause an infaunal bloom instead (Thomson et al., 1988; Smith et al., 1993). In addition, the thinner beds are simply not of sufficient scale in some cases to avoid significant overprinting and obscuration by bioturbation at even average background levels. This is the primary reason that multiple cores at a given site are desirable, because these artifacts in any single core can by identified as "noise" with multiple cores, but can be misleading when considered in only one core. Another factor is that geophysical grain size proxies may break down to some extent at small grain sizes. This is because the biogenic content of the mud turbidites is higher, and some of the microfossil content is larger than the mineral grain and clay matrix, causing the geophysical proxies to be less responsive to these beds. The original logging of the mud beds as darker hemipelagic sediment was largely out of context because the entire core set was not available to examine at once. It was only after considerable examination and lab work, and a number of correlation attempts that continuity was established between these anomalous beds among the Rogue Apron cores. Addition of the 2009 core TN0909-01JC/TC solidified these linkages as they were replicated precisely in this core, which is several km more distal than the original 1999 Rogue cores.

Brunner and Normark (1985) and Brunner and Ledbetter (1985, 1987, 1989) closely examined biostratigraphy of mud turbidites in an effort to define both mechanical and faunal discriminators to identify mud turbidites. Although they were largely successful, they also caution that such discriminators are highly subject to local physiography and the local hydrodynamics in terms of the evidence left behind in each deposit. These types of faunal counting and fabric analysis techniques are exceptionally labor intensive, and ultimately may or may not be definitive, therefore multiple proxies and correlation techniques are likely more effective in practice.

Although the mud-silt turbidites of southern Cascadia were commonly difficult to date at Rogue Apron and have weak physical-property signatures, they are observed persistently at similar stratigraphic intervals in cores between Hydrate Ridge and Trinidad Plunge Pool. These beds occur at approximately the same frequency and at similar times to many smaller events recorded onshore at the Bradley Lake, Sixes River, and Coquille River coastal paleoseismic sites, and potentially at other inland lakes. In particular, the correlation between Hydrate Ridge and Rogue Apron supports the interpretation of the smaller mud turbidites as earthquake generated, as significant coincidence would be required to generate the two similar sequences by some other mechanism.

Bradley Lake appears to be a good match for the offshore southern Cascadia record, although it appears to be somewhat less sensitive to minimum earthquake size than the offshore turbidite record, but much more sensitive than other land sites. The evidence for tsunami entering

Bradley Lake at times that correspond to some of the offshore turbidites, but do not correspond to regional margin-wide earthquakes provides a third independent line of evidence for additional smaller earthquakes in southern Cascadia. Cascadia earthquakes recorded in Bradley Lake must also meet the requirement to generate a tsunami height of ~ 5.5 m to overtop the barriers to Bradley Lake (Kelsey et al., 2005), which likely excludes slab and upper plate earthquakes. The evidence of turbidites in four lakes onshore in southern Cascadia extends this line of evidence to eight sites in southern Cascadia: one barrage lake, three marsh sites, and four inland lakes. Among the coastal sites at Bradley Lake, Coquille River, Sixes River, and the Humboldt Bay area, temporal equivalents exist for 11 of the 17 Rogue thin beds for the period 0-6500 cal BP, or 65% of the offshore thin beds at similar latitudes. Of these 11, 6 are inferred at one site, three at two sites, three are evident at three sites, and none are evident at all four coastal sites. The four inland lakes cover different time ranges, with only one of them (Sanger Lake) spanning the time range considered here (0-6500 cal BP). Even so, the aggregate of the most robust equivalents includes 15 of the 17 thin beds at Rogue Apron for that period. Four of these fifteen events found in the inland lakes but are not represented at coastal sites, while eleven are evident at both. Considering all eight coastal and inland sites, we infer that earthquake evidence and lake turbidites with temporal equivalents offshore may account for 15 of 17 events in this period, or 88%. Of these fifteen events, shows that five are evident at one site, six are evident at two sites, three are evident at three sites, and one (T5b) is evident at five sites. Presently, not enough evidence exists from central and northern Cascadia lakes and onshore paleoseismic sites to corroborate northward terminations interpreted from the existing onshore-offshore evidence (Goldfinger et al., 2012).

With respect to the preliminary lake records, we suggest that great earthquakes are the only forcing likely to have generated deposits with such similarity in physical properties, event frequency and chronology by destabilizing sediments within the lakes and creating a subaqueous sediment flow similar those generated in the marine environment. We note that the overall sedimentation rate in these lakes is quite high, enough so that a mechanism other than normal drainage sedimentation may be required. We suggest that drainage events, possibly also triggered by earthquakes, move sediment downslope toward the lakes in interseismic times more quickly than might occur otherwise, "reloading" the sediment failure zones that are likely triggered during earthquakes (i.e. Dadson et al., 2004, 2005). This process may closely parallel the marine process offshore, where coastal rivers reload the offshore canyon heads simultaneously (Sommerfield and Nittrouer, 1999; Sommerfield and Wheatcroft, 2007, Puig et al., 2004).

The continuity of seismic reflectors in the Holocene section along 240 km of the abyssal plain centered on Rogue Apron was surprising to us. Both the lack of thickening of the section at the Rogue Canyon mouth, and the continuity of the reflectors along strike suggest that the delivery of turbidites to the southern Cascadia abyssal plain may be accomplished by sheet flows from the lower continental slope.

The 21 correlated thin turbidites and the 2 thicker ones represent an average recurrence interval of ~430 years. The long interval suggests that alternative triggers, such as major storm events, are unlikely for many of the same reasons that apply to the larger turbidites discussed in more detail in Goldfinger et al. (2012). In sum, we reiterate that the thin mud turbidites are most likely impulsive turbidites as opposed to storm-generated events. The evidence for correlation between Hydrate Ridge and Rogue Apron is best explained by smaller earthquakes of limited rupture length, though with fewer tests of origin than available for the marginwide turbidites. In addition to the intersite correlation, the preferred interpretation of the presence of these smaller

turbidites at Hydrate Ridge places an additional constraint on possible origins in that shallow-water origins, such as storm or tsunami triggering are excluded at the isolated Hydrate Ridge site. The interpretation of the thinner beds presented in Goldfinger et al. (2012) is supported and extended southward more robustly using 2009 cores. Though the age control is not yet as complete as Rogue Apron, evidence thus far suggests that most of the thin beds at Rogue coarsen southward, many becoming sandy turbidites.

In summary, we reiterate the interpretation of three southern Cascadia segments in addition to the full margin ruptures represented by T1–T18 (Goldfinger et al., 2012, their Figure 55). To this interpretation, we have added one possible turbidite limited to the northern margin, called T15AN. We note that a small number of uncorrelated turbidites are also present in some of our proximal cores such as the Hydrate Ridge cores 56PC and 02PC. These uncorrelated beds are not common, and limited to very proximal sites. They may be the result of random self-failures, or perhaps small local earthquakes. In Southern Cascadia, south of the Rogue Canyon system, the turbidite record includes a stepwise increase in turbidite frequency toward the Mendocino Triple Junction. Though the evidence for southern Cascadia segmented ruptures is now stronger, the southernmost margin remains difficult to interpret. The turbidite record, particularly south of Trinidad Plunge Pool, may result from numerous seismic sources, additional seismic segments, and possibly inclusion of storm events related to the high sediment discharge Eel River, which is anomalously close (12 km) to the shelf edge and Eel Canyon (Goldfinger et al., 2012, Puig et al., 2004). North of Trinidad Plunge Pool, our preferred model is that the correlated turbidites are most likely generated from plate boundary earthquakes because of the > 150 km strike length over which they are observed, but we are unable to rule out very large upper plate or Gorda Plate earthquakes.

NSAF Turbidites

The Northernmost Sand Andreas cores on which we are focusing were considerably simpler than the southern Cascadia cores to which we are comparing. The original cores from Noyo channel/Canyon 48PC/TC, 49PC/TC and 54KC, compare well to the new R/V Thompson cores TT0909-14 and 15PC/TC, 25KC. Correlation was straightforward and presented few difficulties. With replicates of these important sites, it became possible to compare the turbidites event for event to resolve questions, develop better hemipelagic intervals, and assess basal differential erosion. One of the most obvious things resolved was the question of events 3 and 4. With the earlier cores, these events appeared to be equally likely to be a single event or two events. The new cores resolved this interval into two events with hemipelagic sediment between the two, where our original core 49PC looked like two events, but no hemipelagic material was found between them. This result, with two events in the time span ~300-450 cal BP is consistent with the Vedanta Marsh paleoseismic record (T. Fumal, pers. Comm. 2007).

We observe that a significant number of Noyo Canyon turbidites are single pulsed. This is in contrast to Cascadia turbidites, where the majority of them are composed of multiple stacked, fining upward sequences. For the NSAF, about 1/3 of the turbidites are multi-pulsed, and 2/3 are uni-pulsed. We suggest that the structural differences may be attributed to the lower magnitudes and accelerations likely from San Andreas earthquakes, simple canyon morphology and perhaps proximal channel location of 49PC in Noyo Channel and 13PC in a Gualala tributary canyon (Pastor et al., 2012). Looking at the whole 13PC in the single Gualala tributary

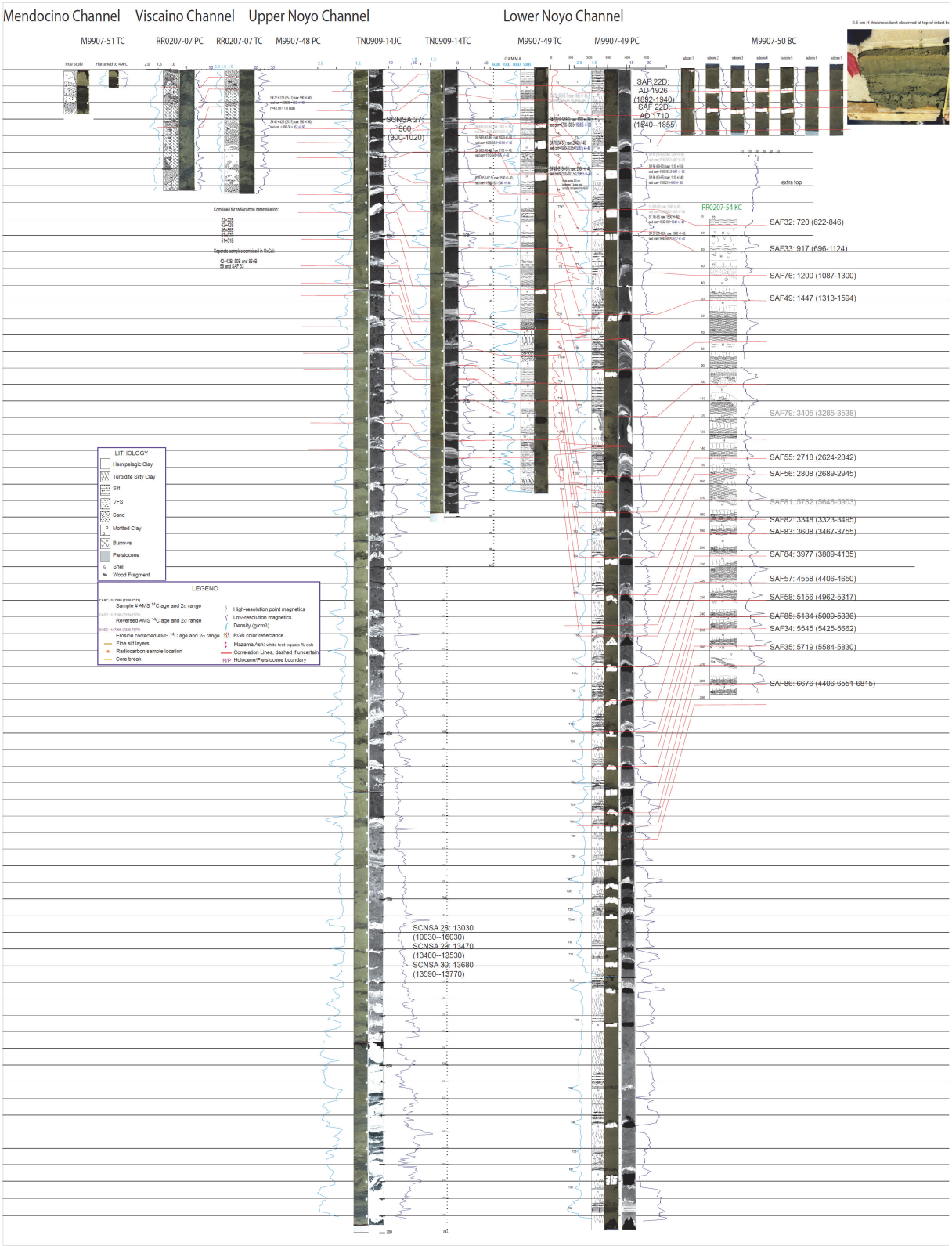

Figure 3. Correlation diagram for the Noyo-Viscaino Channel region of the NSAF with 1999, 2002, and 2009 cores shown. Radiocarbon data for new ages fromthis project shown in this figure and Figure 2 are given in Table 1.

canyon we find that 9 turbidites are uni-pulsed and two uni-pulsed turbidites may have weak multiple pulses (Goldfinger et al., 2007). The dominance of uni-pulsed turbidites in Noyo channel and Gualala tributary canyon suggests that the generally weaker earthquakes of northern California margin (≤ 8 Mw) may generate dominantly uni-pulsed turbidites in proximal tributary canyons and channels with simple morphology (i.e. without other tributaries). Additionally, the strongest NSAF earthquakes may be responsible for the few multi-pulsed turbidites (Goldfinger et al., 2007). For example, the turbidite associated with the 1906 earthquake is sampled in several cores, and is clearly a two pulse event, and thus in the minority for the NSAF. Garrett et al. (2011) have suggested that the turbidite matches the 1906 earthquake itself, which had two main rupture patches north of the Golden Gate (Song et al., 2008). This is a speculative conclusion, and other factors may be involved. For example, The NSAF is a nearly vertical, linear fault that is fundamentally very different seismic source that a shallow dipping subduction zone. We suspect that the spatial patterns of shaking from a lengthy subduction zone earthquake are much more likely to generate temporal heterogeneity of the earthquake source, and possible result in longitudinal heterogeneity in the resulting turbidity current. If the turbidites are reflective of the seismic source (see Goldfinger et al., 2008; 2012), this may explain the differences between Cascadia and NSAF turbidites.

Abrupt Changes to Sediment Supply Along the Offshore NSAF

Cores to the south of Noyo Canyon/Channel have much reduced sedimentation rates, even though they are closer to the Russian River source, the largest river along the North Coast section of the NSAF. In our 2008 BSSA paper we speculated that the low hemipelagic sedimentation rates might be related to capture of much of the Russian River drainage and diversion into the San Joaquin Valley, which may have occurred during the Holocene (Mauldin 1968, Hopkirk, 1973; 1988). By comparison to the robust Noyo record, most of the events along the NSAF in other channels are subdued, and indeed the upper 10 events shown in these figures are very fine silt turbidites not visible to the naked eye. Their unique signatures in the physical property data, however, allowed reasonable correlation between sites south of Noyo. The hypothesis, originally based on a specie of perch found in both the Russian River and the San Joaquin River, suggested that Clear lake once drained into both rivers. The hypothesis is well supported by genetic studies of the fish, which require a common recent origin. Although beyond the scope of this project, we examined this area in the field to do a reconnaissance investigation of this hypothesis due to its impact on the offshore turbidite record. We found that Clear Lake did on fact drain to the north into a tributary of the Russian River at Blue Lakes. Blue Lakes are a series of three small lakes on this river outlet in Cold Creek Canyon which was dammed by the Blue Lakes landslide. The landslide is very apparent based on the hummocky morphology, the lobate planform, and the chaotic nature of the deposit itself. The landslide scar of the "Cow Mountain" slide west of Highway 20 is apparent, and the slide clearly blocked Cold Creek. We estimated that the age of this landslide and drainage change of Clear Lake, would have been ~ 2500 years ago in order to account for the sedimentation rate changes we observe offshore. Informal sources (Enderlin, 2007) suggest that an age of a few thousand years is consistent with Native American oral traditions that include the Cow Mountain landslide and drainage change of Clear Lake. Much of the physiography of the slide was reported in Holway (1907). Our observations agree with these observations in that the slide clearly crossed the valley and ran somewhat up the opposite side. Slide debris is in direct contact with the local canyon wall rock on the east side. Holway reported no apparent difference in age of the trees on

ones side of the canyon vs. the other in 1907, and we could also see no difference. We did observe clear evidence of subsequent continuing downslope movement, and many stands of trees on the Blue Lakes road side of the slide are leaning strongly downslope.

Mike Rymer and John Sims mapped the slide (Rymer and Sims, 1975) and reported to us that he met some soil scientists working in the area many years ago, and that they thought the slide was around 3000 years old based on the overlying soils. Any reports or publications on this topic have not been found. On the other hand, Bob MacPherson (Humboldt State University) considers the Cashe Creek outlet to have been active for 10-13000 years, suggesting a slightly pre-Holocene age for the Cow Mountain Slide.

We did not collect samples or attempt to date the slides, thus our observations do not add any constraints to it age, but this possibility exists and should be pursued.

Non-Technical Summary

Cores from Noyo Channel on the ocean floor off northern California, and cores off southern Oregon in several channels have been studied for sand layers. These sand layers are thought to represent times when great earthquakes on the northern San Andreas Fault and southern Cascadia subduction Zone have shaken the continental margin, resulting in landslides that transport the sand down the channels. We have determined the ages of many these layers, and these ages suggest that major earthquakes have occurred on average every ~ 200 yr for the past ~ 3000 years. We are refining the timing and continuity of these layers to determine if earthquakes on both faults may have occurred at the same or nearly the same time, indicating one fault may have triggered the other.

Published Results to Date

Goldfinger, C., Morey, A., Erhardt, M., Nelson, C.H., Gutiérrez-Pastor, J., Enkin, R., and Dallimore, A. 2006, Cascadia Great Earthquake Recurrence: Rupture Lengths, Correlations and Constrained OxCal Analysis of Event Ages, proceedings of the USGS Tsunami Sources Workshop, Diggles, J., Geist, E., and Lee, H., eds. CD-ROM, April 21 and 22, 2006.

Goldfinger, C., Morey-Ross, A., Erhardt, M., Nelson, C.H., Johnson, J.E., Guiterrez-Pastor, J., 2005, Cascadia great earthquake recurrence: rupture lengths, correlations and constrained OxCal analysis of event ages, Eos Trans. AGU (Fall Meeting Suppl., Abstract 246TT13.

Goldfinger, C., Morey, A., Nelson, H., Deep-water turbidites as Holocene earthquake proxies along the Northern San Andreas Fault system, 2006, Seismol. Res. Lett. 77 (2) (2006) 195–196.

Goldfinger, C., Morey, A., Nelson, C.H., Gutierrez-Pastor, J., Johnson, J.E., Karabanov, E., Chaytor, J., Eriksson, A., and the Shipboard Scientific Party, 2007, Rupture Lengths and Temporal History of Significant Earthquakes on the Offshore and North Coast Segments of the Northern San Andreas Fault Based on Turbidite Stratigraphy: Earth and Planetary Science Letters, v. 254, p. 9-27.

Goldfinger C., Nelson, C.H., Gutierrez-Pastor, J., Morey-Ross, A, Johnson, J., Chaytor, J., Ericsson, D., Karabanov, Eugene and the 37 members Shipboard and Scientific Party, 2005. Holocene Seismicity of the N. San Andreas Fault based on precise dating of the turbidite event record, USGS NEHRP Workshop, 2nd Annual Northern California Earthquake Hazards, Research Summaries FY 2004, Menlo Park, California.

Goldfinger, C., Nelson, C. H., Johnson, J. E., 2001. Holocene Seismicity of the Northern San Andreas Fault Based on the Turbidite Event Record: Seismological Research Letters, v. 72.

Goldfinger, C., Nelson, C. H., and Johnson, J. E., 2001, Temporal patterns of turbidites offshore the Northern San Andreas Fault and correlation to paleoseismic events onshore: EOS, Transactions of the American Geophysical Union, v. 82, p. F934.

Goldfinger, C., Nelson, C.H, and Johnson, J. E, 2005. Deep-Water Turbidites as Holocene Earthquake Proxies: The Northern San Andreas Fault System, USGS NEHRP Workshop, 2nd Annual Northern California Earthquake Hazards, Research Summaries FY 2004,Menlo Park, California.

Goldfinger, C., Nelson C. H., Johnson, J. E., Shipboard Scientific Party, 2003. Deep-Water Turbidites as Holocene earthquake proxies: The Cascadia Subduction Zone and northern San Andreas fault systems: Annals of Geophysics, v. 46, p 1169-1194.

Goldfinger, C., Nelson, C. H., Johnson, J., Shipboard Scientific Party, 2003. Holocene Earthquake Records From The Cascadia Subduction Zone And Nothern San Andreas Fault Based On Precise Dating Of Offshore Turbidites: Ann. Rev. Earth Planet. Sci. v. 31, p 555-577.

Goldfinger C. , Nelson, H. C., Morey-Ross, A., Gutierrez-Pastor, J., Johnson, J., Chaytor, J., Ericsson, D., Karabanov, Eugene and the 37 members Shipboard and Scientific Party, 2005. Turbidite Paleoseismology of the Cascadia Subduction Zone and northern San Andreas Fault, International Symposium on Active Faulting, Hokudan, Japan.

Gutierrez-Pastor, J., Nelson C.H., Goldfinger C., Johnson J. E., 2004, Turbidite Stratigraphy on active tectonic margins and implications for Holocene paleoseismicity of the Cascadia Subduction Zone and northern San Andreas Fault: 32 nd Int. Geol. Congr. Abs. Vol., pt. 2, Abs. 265-5, p.1193.

Goldfinger, C., Morey, A.E., Nelson, C.H., Gutiérrez-Pastor, J., Johnson, J.E., Karabanov, E., Chaytor, J., Ericsson, A., and shipboard scientific party, 2007, *Rupture lengths and temporal history of significant earthquakes on the Offshore and Northcoast segments of the Northern San Andreas Fault based on turbidite stratigraphy*, Earth and Planetary Science Letters, v. 254, p. 9-27.

Goldfinger, C., Grijalva, K., Burgmann, R., Morey, A.E., Johnson, J.E., Nelson, C.H., Gutierrez-Pastor, J., Karabanov, E., Chaytor, J.D., Patton, J., and Gracia, E., 2008, *Late*

Holocene Rupture of the Northern San Andreas Fault and Possible Stress Linkage to the Cascadia Subduction Zone, Bulletin of the Seismological Society of America, v. 98, p. 861-889.

Goldfinger, C., Patton, J.R., Morey, A.M., 2009, Reply to comment on "*Late Holocene Rupture of the Northern San Andreas Fault and Possible Stress Linkage to the Cascadia Subduction Zone*, Goldfinger, C., Grijalva, K., Burgmann, R., Morey, A., Johnson, J.E., Nelson, C.H., Ericsson, A., Gutiérrez-Pastor, J., Patton, J., Karabanov, E., Gracia, E.", Bulletin of the Seismological Society of America, v. 98, p. 861-889, 8 pp.

Goldfinger, C., 2009, *Subaqueous Paleoseismology*, *in* Mcalpin, J., ed., *Paleoseismology*, 2nd edition, Elsevier, p. 119-169.

Goldfinger, C., 2011, *Submarine Paleoseismology Based on Turbidite Records*, Annual Reviews of Marine Science, v. 3, p. 35-66.

Goldfinger, C., Nelson, C.H., Morey, A., Johnson, J.E., Gutierrez-Pastor, J., Eriksson, A.T., Karabanov, E., Patton, J., Gracia, E., Enkin, R., Dallimore, A., Dunhill, G., and Vallier, T., 2012, *Turbidite Event History: Methods and Implications for Holocene Paleoseismicity of the Cascadia Subduction Zone*, USGS Professional Paper 1661-F, Reston, VA, U.S. Geological Survey, p. 184 p, 64 Figures. . http://pubs.usgs.gov/pp/pp1661f/

Goldfinger, C., Ikeda, Y., Yeats, R.S., and Ren, J., 2013, in press, Superquakes and Supercycles, Seismological Research Letters. V. xx. p. xx-xx.

Goldfinger, C., Morey, A., Black, B., Beeson, J. and Patton, J., 2012, in revision, Spatially Limited Mud Turbidites on the Cascadia Margin: Segmented Earthquake Ruptures?, *in* Pantosti, D., Gracia, E., Lamarche, G., Nelson, C.H., and Tinti, S., eds., Research Conference Submarine Paleoseismology: The Offshore Search of Large Holocene Earthquakes: Obergurgl, Austria, Natural Hazards and Earth System Sciences.

Gutierrez-Pastor, J., Nelson, H.C., Goldfinger C., and Johnson, J.E., 2005, Holocene turbidite history in the Cascadia Subduction Zone shows the potential to develop paleoseismicic methods for the Sumatra and other subduction zones, Vienna (abs.): European Geophysical Union Meeting 05, A07873.

Gutierrez-Pastor, J., Nelson,H. C., Goldfinger C., Johnson, J. E., 2005. Holocene turbidite and onshore paleoseismic record of great earthquakes on the Cascadia Subduction Zone: relevance for the Sumatra 2004 Great Earthquake.*Eos Trans. AGU, 86*(18), Jt. Assem. Suppl.,Abstract U51A-03.

Gutierrez-Pastor, J., Nelson, C. H., Goldfinger, C., and Johnson, J.E., Escutia, C., Eriksson, A., and Morey, A. and The Shipboard Scientific Party, 2006, Earthquake Control and Holocene Turbidite Recurrence on the Cascadia and Northern California Active Continental Margins (Western North America), GS/SEPM Conference "External Controls on Deep-Water Depositional Systems, Abstracts volume, Geological Society, London.

Gutierrez-Pastor, J., Nelson, C. H., Goldfinger, C., and Johnson, J.E., Escutia, C., Eriksson, A., and Morey, A. and The Shipboard Scientific Party, in press, Earthquake Control and Holocene Turbidite Recurrence on the Cascadia and Northern California Active Continental Margins (Western North America), GS/SEPM, Special Publication "External Controls on Deep-Water Depositional Systems", Editors: Ben Kneller, Bill McCaffrey and Ole J. Martinsen. 30p.

Morey-Ross, A., Goldfinger, C., Nelson, C.H., Chaytor, J., Johnson, J.E., Ericsson, E., and the Shipboard Scientific Party, 2003, Turbidite Based Earthquake Record Along the Northern San Andreas Fault: Eos, Trans.AGU, 84 (46), Fall Meet.Suppl. Abstract, T51C-02.

Morey-Ross, A., Goldfinger, C., Erhardt, M., Nelson, C.H., Johnson, J.E., Gutierrez-Pastor, J., 2006, Northern San Andreas Earthquake Recurrence: Rupture lengths, correlations and constrained OxCal analysis of event ages Eos Trans. AGU, Fall Meet .Supp.., Abstract, 247 TT01.

Nelson, C.H., Escutia, C., Karabanov, E., Goldfinger,C., Johnson, J., Gutierrez-Pastor, J., 2006, Tectonic, volcanic, sedimentary, climatic, sea level, oceanographic, and anthropogeniccontrols on turbidite systems, Society for Sedimentary Geology, GS/SEPM, Conference on "External Controls on Deep-Water Depositional Systems, Abstracts volume, Geological Society, London.

Nelson, C.H., Escutia, C., Karabanov, E., Goldfinger,C., Johnson, J., Gutierrez-Pastor, J., 2006, Tectonic, volcanic, sedimentary, climatic, sea level, oceanographic, and anthropogeniccontrols on turbidite systems, Society for Sedimentary Geology, GS/SEPM, Conference on "External Controls on Deep-Water Depositional Systems, Editors: Ben Kneller, Bill McCaffrey and Ole J. Martinsen. 35p.

Nelson, C. H., and Goldfinger, C., 2000. Turbidite event stratigraphy: implications for Holocene Paleoseismicity of the Cascadia Subduction Zone and northern San Andreas Faults. EOS, Transactions of the American Geophysical Union, v. 81, p1224.

Nelson C. H., Goldfinger C., Johnson J., Dunhill G., Gutierrez- Pastor J., Vallier T. L., Kashgarian M., McGann M. L, in review, Turbidite event history, methods and implications for Holocene paleoseismicity of the Cascadia Subduction Zone, *U.S. Geological Survey and Professional Paper*, 1661C, 200 p.

Nelson C. H, Goldfinger C., Gutierrez-Pastor J., Johnson J. E. 2004. Holocene turbidite recurrence frequency off northern California: insights for San Andreas fault paleoseismicity: EOS Trans. AGU, *Fall Meet .Suppl*. Abstract T12B-08.

Nelson, C.H., Goldfinger, C., Gutierrez-Pastor, J., Johnson, J. E., 2005.Cascadia Subduction Zone: confirmation by onshore records and the Sumatra 2004 Great earthquake.European Geophysical Union Meeting 05, Vienna, A07269.

Nelson C.H., Goldfinger, C., Karavanov, E., Gracia, E., Johnson, J. E., Ericksson, D., Chaytor, J., et.al., 2003. Sand-Rich Holocene Turbidite Systems Along the Active Transform Fault Margin of Northern California, AAPG Annual Meeting Official Program, v. 12, p. A127.

References Cited

Aagaard, B.T., Brocher, T.M., Dolenc, D., Dreger, D., Graves, R.W., Harmsen, S., Hartzell, S., Larsen, S., McCandless, K., Nilsson, S., Petersson, N.A., Rodgers, A., Sjögreen, B., and Zoback, M.L., 2008, Ground-Motion Modeling of the 1906 San Francisco Earthquake, Part II: Ground-Motion Estimates for the 1906 Earthquake and Scenario Events Bulletin of the Seismological Society of America, v. 98, p. 1012 - 1046.

Abdeldayem, A.L., Ikehara, K., and Yamazaki, T.: Flow path of the 1993 Hokkaido-Nansei-oki earthquake seismoturbidite, southern margin of the Japan sea north basin, inferred from anisotropy of magnetic susceptibility: Geophys. Jour. Int., 157, 15–24, 2004.

Abrams, L.J.: Correlation among core, logging, and seismic data at Site 1149 in the Nadezhda Basin, *in* Ludden, J.N., Plank, T., and Escutia, C. (Eds.), *Proc. ODP, Sci. Results,* 185 [Online]. http://www-odp.tamu.edu/publications/185_SR/001/001.htm, 2002.

Bett, B.J. and Rice, A.L.: The influence of hexactinellid sponge (*Pheronema carpenteri*) spicules on the patchy distribution of macrobenthos in the Porcupine Seabight (bathyal NE Atlantic): Ophelia, 36, 217–226, 1992.

Blott, S.J., and Pye, K.: Particle size distribution analysis of sand-sized particles by laser diffraction—An experimental investigation of instrument sensitivity and the effects of particle shape: Sedimentology, 53, 671–685, 2006.

Brunner, C.A., and Ledbetter, M.T.: Hydraulic sorting of foraminifers in visually undetected turbidites in late Pleistocene sediments of Monterey Fan on the Central California continental margin: The Geol. Soc. of Am.; 98th annual meeting Abstracts with Programs – Geol. Soc. of Am., 17: Orlando, FL United States, 533, 1985.

Brunner, C.A., and Ledbetter, M.T.:, Sedimentological and micropaleontological detection of turbidite muds in hemipelagic sequences; an example from the late Pleistocene levee of Monterey Fan, Central California continental margin: Mar. Micropaleo., 12, 223-239, 1987.

Brunner, C.A., and Ledbetter, M.T.:Late Quaternary quantitative planktonic foraminiferal biostratigraphy in turbidite sequences of the Central California continental margin: Micropaleo., 35, 321-336, 1989.

Brunner, C.A., and Normark, W.R.: Biostratigraphic implications for the turbidite depositional processes on the Monterey deep-sea fan, Central California: Jour. of Sed. Pet., 55, 495-505, 1985.

Chen, Y., Hur, H., Leigh, J., Johnson, A., Renambot, L., Ito, E., Morin, P., Higgins, S., Reed, J.: The CoreWall Project - Core Visualization, Stratigraphic Correlation and Rich Media Distribution, Workshop on "the Future of Continental Scientific Drilling, a US Perspective", Denver, Colorado, June 2009.

Dadson, S.J., Hovius, N., Chen, H., Dade, W.B., Lin, J.C., Hsu, M.L., Lin, C.W., Horng, M.J., Chen, T.-C., Milliman, J., Stark, C.P.: Earthquake-triggered increase in sediment delivery from an active mountain belt, Geology 32, 733–736, 2004.

Dadson, S.J., Hovius, N., Pegg, S., Dade, W.B., Horng, M.J., Chen, H.: Hyperpycnal flows from an active mountain belt, Jour. Geophys. Res., 110, F04016. doi:10.1029/2004JF000244, 2005.

Fukuma, K.: Origin and applications of whole-core magnetic susceptibility of sediments and volcanic rocks from Leg 152: *Proc. ODP, Sci. Results*,152, 271-280, 1998.

Garrett, A., Goldfinger, C., Paton, J., Morey, A.: "Paleoseismograms": Testing a Hypothesis of Source-Time Function Recording of Paleoearthquakes, AGU Fall Meeting, Abstract T51F-2421. E-poster: http://activetectonics.coas.oregonstate.edu/paper_files/posters/garrett_agu_poster_final.pdf., 2011.

Goldfinger, C., Nelson, C.H., and Johnson, J.E.: Deep-water turbidites as Holocene earthquake proxies: The Cascadia Subduction Zone and northern San Andreas fault systems, Annali Geofisica, 46, 1169–1194, 2003a.

Goldfinger, C., Nelson, C.H., and Johnson, J.E.: Holocene earthquake records from the Cascadia Subduction Zone and northern San Andreas fault based on precise dating of offshore turbidites: Ann. Rev. Earth and Plan. Sci., 31, 555–577, 2003b

Goldfinger, C., Morey, A.E., Nelson, C.H., Gutierrez-Pastor, J., Johnson, J.E., Karabanov, E., Chaytor, J., and Ericsson, A.: Rupture lengths and temporal history of significant earthquakes on the offshore and north coast segments of the northern San Andreas fault based on turbidite stratigraphy: Earth and Plan. Sci. Lett., 254, 9–27, 2007.

Goldfinger, C., Grijalva, K., Burgmann, R., Morey, A.E., Johnson, J.E., Nelson, C.H., Gutierrez-Pastor, J., Karabanov, E., Chaytor, J.D., Patton, J., and Gracia, E.: Late Holocene Rupture of the Northern San Andreas Fault and Possible Stress Linkage to the Cascadia Subduction Zone: Bulletin of the Seis. Soc. Am., 98, 861–889, 2008.

Goldfinger, C.: Possible turbidite record of earthquake source characteristics: a small scale test, NEHRP Annual Report, 34: Reston, VA, U.S. Geological Survey, 18p, 2011.

Goldfinger, C., Nelson, C.H., Morey, A., Johnson, J.E., Patton, J., Karabanov, E., Gutierrez-Pastor, J., Eriksson, A.T., Gracia, E., Enkin, R., Dallimore, A., Dunhill, G., and Vallier, T.: Turbidite Event History: Methods and Implications for Holocene Paleoseismicity of the Cascadia Subduction Zone, U.S. Geological Survey Professional Paper 1661-F, Reston, VA, U.S. Geological Survey,184p, 64 Figures, 2012.

Goldfinger, C., Morey, A., Black, B., Beeson, J. and Patton, J., 2013, in revision, Spatially Limited Mud Turbidites on the Cascadia Margin: Segmented Earthquake Ruptures?, *in* Pantosti, D., Gracia, E., Lamarche, G., Nelson, C.H., and Tinti, S., eds., Research Conference Submarine Paleoseismology: The Offshore Search of Large Holocene Earthquakes: Obergurgl, Austria, Natural Hazards and Earth System Sciences.

Henkart, P.: Chirp Sub-Bottom Profiler Processing - A review: Sea Technology, 35-38, 2006.

Holway, R.S., 1907, Physiographic Changes Bearing on the Faunal Relationships of the Russian and Sacramento Rivers, California, Science, New Series, v. 26, No. 664 (Sep. 20, 1907), pp. 382-383.

Hopkirk, J. D. 1973. Endemism in Fishes of the Clear Lake Region. Univ. Calif. Pub. Zool. 96, 160 pp. Hodges, C. --- Geomorpholoqy of Clear Lake. Unpub. Ph.D. Thesis, Stanford University, Stanford, Calif.

Iwaki, H., Hayashida, A., Kitada, N., Ito, H., Suwa, S., and Takemura, K.: Stratigraphic correlation of samples from the Osaka Bay off Kobe based on magnetic properties and its implication for tectonic activity of the Osaka-wan fault for the last 6300 years, Eos Trans. Am. Geophys. Union, 84, GP41C-0053 F554, 2004.

Karlin, R.C., and Abella, S.E.B.: Paleoearthquakes in the Puget Sound region recorded in sediments from Lake Washington, U.S.A., Science, 258, 1617–1620, 1992.

Karlin, R.E., Holmes, M., Abella, S.E.B., and Sylwester, R., 2004, Holocene landslides and a 3500-year record of Pacific Northwest earthquakes from sediments in Lake Washington, Geol. Soc. Am. Bull., 116, 94–108, 2004.

Kelsey, H.M., Nelson, A.R., Hemphill-Haley, E., and Witter, R.C.: Tsunami history of an Oregon coastal lake reveals a 4600 yr record of great earthquakes on the Cascadia subduction zone, Geol. Soc. Am. Bull., 117,1009–1032, 2005.

King, J., Banerjee, S.K., Marvin, J., and Özdemir, Ö., 1982, A comparison of different magnetic methods for determining the relative grain size of magnetite in natural materials: Some results from lake sediments: Earth and Planetary Science Letters, v. 59, p. 404-419.

Kneller, B., and Buckee, C., 2000, The structure and fluid mechanics of turbidity currents: a review of some recent studies and their geological implications: Sedimentology, v. 47, p. 62-94.

Lovlie, R., and Van Veen, P.: Magnetic susceptibility of a 180 m sediment core: reliability of incremental sampling and evidence for a relationship between susceptibility and gamma activity, *in* Turner, P., and Turner, A., eds., Palaeomagnetic applications in hydrocarbon exploration and production: Special Publication, 98, Geological Society, London, 259–266, 1995.

McCubbin, D.G.: Barrier-island and strand-plain facies, *in* Scholle, P.A., and Spearing, D., eds., Sandstone Depositional Environments, Memoir 31, AAPG, 247-258, 1982.

Gutierrez-Pastor, J., Nelson, C.H., Goldfinger, C., Johnson, J.E., Escutia, C., Eriksson, A., and Morey, A., 2009, Earthquake Control of Holocene Turbidite Frequency Confirmed by Hemipelagic Sedimentation Chronology on The Cascadia and Northern California Active Continental Margins, *in* Kneller, B., Martinsen, O.J., and McCaffrey, W., eds., External Controls on Deep-Water Depositional Systems, Volume 92: London, Society for Sedimentary Geology p. 179-196.

Patton, J.R., Goldfinger, C., Morey, A., Erhardt, M., Black, B., Garrett, A.M., Djadjadihardja, Y.S., and Hanifa, U.: 7.5 ka earthquake recurrence history in the region of the 2004 Sumatra-Andaman earthquake, Geol. Soc. Am. Abstracts with Programs, 41, 408, 2009.

Puig, P., Ogston, A.S., Mullenbach, B.L., Nittrouer, C.A., Parsons, J.D., and R. W. Sternberg, R.W.: Storm-induced sediment gravity flows at the head of the Eel submarine canyon, northern California margin, Jour. Geophys. Res., 109, C03019, 2004.

Ramsey, C.B.: Development of the radiocarbon program OxCal, Radiocarbon, 43, 355–363, 2001.

Rymer, M.J. and Sims, J.D., 1975, Preliminary photo interpretation map of landslides and other surficial deposits in the Cow Mountain 7.5′ Quadrangle, Lake and Mendocino counties, California, U.S. Geological Survey Miscellaneous Field Studies Map MF-680, scale 1:24,000.

Schnellmann, M., Anselmetti, F.S., Giardini, D., and Ward, S.N.: Prehistoric earthquake history revealed by lacustrine slump deposits, Geology, 30, 1131-1134, 2002.

Smith, C.R., Pope, R.H., DeMaster, D.J., and Magaard, L.: Age-dependent mixing of deep-sea sediments, Geochimica et Cosmochimica Acta, 57, 1473–1488, 1993.

Sommerfield, C.K., Nittrouer, C.A.: Modern accumulation rates and a sediment budget for the Eel shelf: a flood dominated depositional environment, Mar. Geol. 154, 227–241, 1999.

Sommerfield, C. K., and Wheatcroft, R. A.: Late Holocene sediment accumulation on the northern California shelf: Oceanic, fluvial, and anthropogenic influences, Geol. Soc. Am. Bull., 119, 9-10, 1120-1134, 2007.

Song, S.G., Beroza, G.C., and Segall, P., 2008, A Unified Source Model for the 1906 San Francisco Earthquake: Bulletin of the Seismological Society of America, v. 98, p. 823-831.

St-Onge, G., Mulder, T., Piper, D.J.W., Hillaire-Marcel, C., and Stoner, J.S.: Earthquake and flood-induced turbidites in the Saguenay Fjord (Québec): a Holocene paleoseismicity record, Quat. Sci. Rev., 23, 283–294, 2004.

Stevenson, C. J., Talling, P. J., Wynn, R. B., Masson, D. G., Hunt, J. E., Frenz, M., Akhmetzhanhov, A., and Cronin, B. T.: The flows that left no trace: Very large-volume turbidity currents that bypassed sediment through submarine channels without eroding the sea floor, Mar. Pet. Geol., in press corrected proof, 2012.

Stuiver, M., and Polach, H.A.: Discussion: Reporting of ^{14}C data, Radiocarbon, 19, 355-363, 1977.

Stupavsky, M., Gravenor, C.P., and Dumala, R., 1976, Technique for measurement of isotropic magnetic susceptibility of till: Geological Society of America Bulletin, v. 87, p. 818-820.

Thomson, J., Colley, J.S., and Weaver, P.P.E.: Bioturbation into a recently emplaced deep-sea turbidite as revealed by 210Pb excess, 230Th excess and planktonic Foraminifera distributions, Earth and Planet. Sci. Lett., 90, 157–173, 1988.

Thomson, J., and Weaver, P.P.E., An AMS radiocarbon method to determine the emplacement time of recent deep-sea turbidites, Sed. Geol., 89, 1–7, 1994.

Tunnicliffe, V., Chapman, R., Yahel, G., and Wilmut, M.: Environmental Impacts of Air-gun Surveys on Glass Sponges, Canadian Ministry of Energy and Mines, 36 pp, 2008.

Wheatcroft, R.A.: Experimental tests for particle size-dependent bioturbation in the deep ocean, Limnol. Ocean., 37, 90-104, 1992.

Wheatcroft, R. A., and Sommerfield, C. K.: River sediment flux and shelf accumulation rates on the Pacific Northwest margin, Cont. Shelf Res., 25, 311-332, 2005.

Data Availability

All processed and raw AMS radiocarbon age data is available in excel tables on request. Analogue records of core lithologic data are archived at the OSU core repository where the cores are stored, as well as the National Geophysical Data Center. More detailed core data and logs are posted as they become available at http://activetectonics.coas.oregonstate.edu/, as are the GIS data base of swath bathymetry, seismic profiles, core locations etc.